# Adsorption of xyloglucan and cellulose nanocrystals on natural fibres for the creation of hierarchically structured fibres

Estelle Doineau, Guillaume Bauer, Léo Ensenlaz, Bruno Novales, Cécile Sillard, Jean-Charles Benezet, Julien Bras, Bernard Cathala, Nicolas Le Moigne

# Adsorption of xyloglucan and cellulose nanocrystals on natural fibres for the creation of hierarchically structured fibres

Estelle Doineau[a,b,c,*,1,2], Guillaume Bauer[c,1], Léo Ensenlaz[b,1,2], Bruno Novales[c,d,1], Cécile Sillard[b,1,2], Jean-Charles Bénézet[a,1], Julien Bras[b,1,2], Bernard Cathala[c,1], Nicolas Le Moigne[a,*,1]

[a] *Polymers Composites and Hybrids (PCH), IMT Mines Ales, Ales, France*
[b] *Univ. Grenoble Alpes, CNRS, Grenoble INP[2], LGP2, F-38000 Grenoble, France*
[c] *INRAE, UR BIA, F-44316, Nantes, France*
[d] *INRAE, BIBS Facility, F-44316 Nantes, France*

A B S T R A C T

Green treatment of natural fibres is a major issue in paper, textile and biocomposites industries to design in-novative and eco-friendly products. In this work, hierarchical structuring of flax woven fabrics by the adsorption of xyloglucan (XG) and cellulose nanocrystals (CNC) is studied. Indeed, CNC have high mechanical properties, high specific surface area and great potential for functionalization. The adsorption of XG and CNC has been investigated in terms of localization by confocal and scanning electron microscopy (SEM) and quantification through adsorption isotherms. Adhesion force measurements have also been performed by Atomic Force Microscopy (AFM). XG and CNC are homogeneously adsorbed on flax fabric and adsorption isotherms reach plateau values around 20 mg /$g_{fibres}$ for both. The pre-adsorption of XG on flax fabric influences the amount of adsorbed CNC in the high concentrations and also creates entanglements and strong interactions between XG and CNC with the formation of an extensible network.

*Keywords:*
Cellulose nanocrystals
Xyloglucan
Flax fibres
Adsorption isotherm

## 1. Introduction

Surface treatments of natural fibres (chemical, physical, enzymatic...) are commonly used in a wide range of industrial sectors like textile, paper or biocomposites to bring them specific properties according to the targeted applications (Kalia, Thakur, Celli, Kiechel, & Schauer, 2013). For instance, in textile applications, surface treatments primarily concern the dyeing and the finishing while in paper industry, surface treatments target functional properties such as printability, bleaching, hydrophobicity, gas barrier, softness, strong mechanical properties. In the more recently developed field of biocomposites, most of the natural fibres surface treatments are developed to improve wettability and compatibility with polymeric matrices. In all these applications, environmental concerns prompt the search and the development of environmental friendly surface treatments procedures in order to decrease the use of polluting chemical products (Araújo, Casal, & Cavaco-Paulo, 2008; Faruk, Bledzki, Fink, & Sain, 2012; Haider, Cho, Moon, & Kim, 2019; Le Moigne, Otazaghine, Corn, Angellier-Coussy, & Bergeret, 2018; Rastogi & Samyn, 2015; Sun, 2016; Wei, 2009).

In the search of innovative and greener surface modifications of natural fibres, functionalization with nanoparticules or biopolymers knows a growing interest (Hajlane, Kaddami, & Joffe, 2017; Dai & Fan, 2013; Hajlane, Joffe, & Kaddami, 2018; Idumah, Ogbu, Ndem, & Obiana, 2019; Lee, Bharadia, Blaker, & Bismarck, 2012; Malik, Kumar, Ghosh, & Shrivastava, 2018; Oksanen, Timo, Retulainen, Salminen, & Brumer, 2011; Zhou, Baumann, Brumer, & Teeri, 2006; Zhuang et al., 2011). With this long term goal, this work proposes to combine adsorption capacity of xyloglucan (XG) on cellulosic substrates with the outstanding properties of cellulose nanocrystals (CNC) to develop hierarchically structured assemblies at the surface of flax woven fabrics. XG is an hemicellulose found in the primary cell wall of plants, which is involved in the wall extensibility and its integrity, through its strong affinity with cellulose microfibrils (Fry, 1989; Fry et al., 1993; Hanus & Mazeau, 2006; Hayashi, Ogawa, & Mitsuishi, 1994; Yong Bum Park & Cosgrove, 2015; Pauly, Albersheim, Darvill, & York, 1999). On the other hand, CNC are used in many applications thanks to their amazing

* Corresponding authors.
*E-mail addresses:* doineau.estelle@orange.fr (E. Doineau), Nicolas.le-moigne@mines-ales.fr (N. Le Moigne).
[1] Members of the European Polysaccharide Network of Excellence (EPNOE), http://www.epnoe.eu.
[2] Institute of Engineering Univ. Grenoble Alpes.

properties (Habibi, Lucia, & Rojas, 2010). They have outstanding mechanical properties, i.e high Young's Modulus estimated between 100 and 150 GPa, a high specific surface area (Dufresne, 2017; Habibi, Chanzy, & Vignon, 2006; Nagalakshmaiah, El Kissi, & Dufresne, 2016; Rusli & Eichhorn, 2008; Yue et al., 2018) and can be chemically functionalized through substitution of their hydroxyl groups. Xyloglucan interactions with cellulosic surfaces have been intensively studied *in vitro* and *in vivo* (1994, Dick-Pérez et al., 2011; Hayashi, Marsden, & Delmer, 1987; Morris, Hanna, & Miles, 2004; Young B. Park & Cosgrove, 2012; Vincken, de Keizer, Beldman, & Gerard Joseph Voragen, 1995), and are known to be an entropy driven process (Benselfelt et al., 2016). From the physico-chemical point of view, glucan chains will interact each other through Hydrogen bonds, van der Waals and polar bonds with some reorganizations of the conformation of XG depending on the polymer concentration (Villares, Moreau, Dammak, Capron, & Cathala, 2015). The final architecture of the cellulose/xyloglucan assemblies is related to concentrations of the building blocks, the molar mass and other adsorption processing parameters (Benselfelt et al., 2016; Dammak, Quémener et al., 2015; Hanus & Mazeau, 2006; Hayashi & Maclachlan, 1984; Hayashi et al., 1987; Lima, Loh, & Buckeridge, 2004; Lopez et al., 2010; Stiernstedt, Brumer, Zhou, Teeri, & Rutland, 2006; Stiernstedt, Nordgren et al., 2006; Vincken et al., 1995). In particular, the strong affinity of XG for cellulose surfaces has attracted researchers for the elaboration of cellulose-based materials as natural cross-linker. For instance, XG and CNC have been already used for the implementation of thin films displaying structural colors or for the reinforcement of nanocellulose aerogels (C. Cerclier, Cousin, Bizot, Moreau, & Cathala, 2010, 2011; C. V. Cerclier et al., 2013; Dammak, Moreau et al., 2015; Jean, Heux, Dubreuil, Chambat, & Cousin, 2009; Sehaqui, Zhou, & Berglund, 2011; Sehaqui, Zhou, Ikkala, & Berglund, 2011).

Ligno-cellulosic fibres properties have also been improved by the adsorption of either XG or nanocellulose. For example, addition of XG by spraying on a bleached birch kraft pulp increases its wet web strength, tension holding, drying tension and also its smoothness (Oksanen et al., 2011). Similarly, when XG is used as a wet end additives in paper making process, paper formation is facilitated and final paper strength is increased (Christiernin et al., 2003; Yan, Lindström, & Christiernin, 2006). In fact, fibre bonds in pulps treated with XG seem to give high adhesion levels. To go further in this way, friction measurements have been performed by AFM between cellulose and XG (Stiernstedt, Brumer et al., 2006; Stiernstedt, Nordgren et al., 2006). These studies show the irreversibility side of the adsorption of XG to cellulose. Moreover, the adhesion between the cellulose surfaces in water, which is often very small, is increased with the presence of XG on the surfaces. It appears that specific bonds are formed between XG and cellulose surfaces, creating a strong bridging between cellulose fibres. Nanocellulose, and more especially bacterial cellulose, has also demonstrated its capacity to increase the strength of the interfacial adhesion between natural fibres and polymeric matrices as reported by Bismarck's group (Fortea-Verdejo, Lee, Zimmermann, & Bismarck, 2016; Juntaro, Pommet, Mantalaris, Shaffer, & Bismarck, 2007; Lee, Bharadia et al., 2012; Lee, Ho, Schlufter, & Bismarck, 2012; Pommet et al., 2008). For example, the creation of "dense" or "hairy" coated sisal fibres via the dipping of sisal fibres in a slurry of bacterial cellulose (BC) has been proposed to reinforce PLA based biocomposites (Lee, Bharadia et al., 2012). The results of this study were promising with an increase of the specific surface area up to 800 % compared to neat sisal fibres. In terms of mechanical properties, the storage modulus of the PLA- BC coated sisal fibres- biocomposite was increased by around 20 % in comparison with PLA-neat sisal fibres. However, up to our knowledge there is no report of combined adsorption of XG and nanocellulose on (ligno-)cellulosic substrates. In this work, the challenge addressed is to characterize the adsorption of XG and CNC on flax fibres and the potential synergistic effect of the combination of the two biobased building blocks. Indeed, similarly to the plant wall architecture, combination of XG and CNC adsorption may yield different to final organization to achieve hierarchical materials combining microscale fibres displaying nanostructured surfaces. Moreover, this study has been achieved on substrates of industrial interest, i.e. flax woven fabrics that present additional levels of complexity when compared to model substrates or unitary natural fibres.

The adsorption of XG and CNC on flax woven fabrics is investigated in terms of localization by confocal and scanning electron microscopy. In order to quantify the adsorbed amount of XG and CNC on flax woven fabrics, adsorption isotherms are established by an UV spectroscopy method. Different adsorption sequences on flax woven fabrics are evaluated: (i) adsorption of XG or CNC (ii) successive adsorption of XG then CNC, (iii) successive adsorption of CNC then XG. Finally, Atomic Force Microscopy (AFM) with XG and CNC modified tips was used to analyze the adhesion between XG, CNC and flax fibres.

## 2. Materials and methods

### 2.1. Materials

A twill $2 \times 2$ flax woven fabric 200 g/m$^2$ was provided by SF Composites (France). Cellulose nanocrystals (CNC) were produced by acid hydrolysis of wood pulp and purchased in spray-dried powder from CelluForce (Quebec, Canada). CNC surface charge density : 0.023 mmol/g; Crystalline fraction : 0.88; CNC lateral dimensions : $2-5$ nm; CNC length : $50-110$ nm. Xyloglucan Glyloid 6 C was obtained from tamarind seed gum and purchased from DSP Gokyo Food & Chemical. $M_w = 840\ 000$ g/mol; $M_w/M_n = 1.24$, $R_g$ 72 nm; monosaccharide composition : Glucose 50.7 %; Xylose 31.7 %; Galactose 16.0 %; Arabinose 1.6 %. Fluorescent agents RBITC (Rhodamine B isothiocyanate) and FITC (Fluoresceine isothiocyanate) were purchased from Sigma-Aldrich.

### 2.2. Labelling of XG and CNC with RBITC and FITC

The fluorescent labelling of XG and CNC were performed according to the method reported by Belder A & Granath K (de Belder & Granath, 1973). The reaction occurring is the formation of covalent bonds between hydroxyl groups of polysaccharides and isothiocyanate groups of the fluorescent agents (Iwakura & Okada, 1962). First, 1 g of CNC or XG was solubilized in 40 mL of DMSO under stirring and heated at 65 °C. After 15 min, few drops of pyridine, 50 µL of dibutyltin dilaurate and 7.5 mg of RBITC (Rhodamine B Isothiocyanate) or FITC (Fluoresceine isothiocyanate) were added. The reaction was heated under stirring at 65 °C during 2 h. XG-RBITC and CNC-RBITC (or CNC-FITC) were recovered by precipitation in ethanol/acetone mixture for XG and NaCl 1 M solution for CNC followed by centrifugation (10 min; 10,000 *g*). Three dispersion/centrifugation cycles were achieved and final precipitates were dissolved / dispersed in deionized water at average concentration of 1 wt% and dialyzed (12–14000 MWCO) during one week against ultrapure water.

### 2.3. Adsorption experiments on flax woven fabrics

The different steps of adsorption experiments are illustrated in Fig. 1 and detailed below.

#### 2.3.1. Simple adsorptions

Small pieces of flax fabrics between 8–12 mg were cut and put in test tubes. To avoid the quenching of RBITC or FITC, all samples need to be in the dark (tubes were wrapped in aluminium film). XG-RBITC or CNC-RBITC solutions of 0.5 g/L were diluted with water in test tubes (final volume 5 mL) to obtain final concentrations ranging between 0.05 g/L and 0.45 g/L. Reference samples were prepared in the same way without flax woven fabrics. Test tubes were gently shaken during 16 h. Other samples were prepared with CNC-FITC in the same

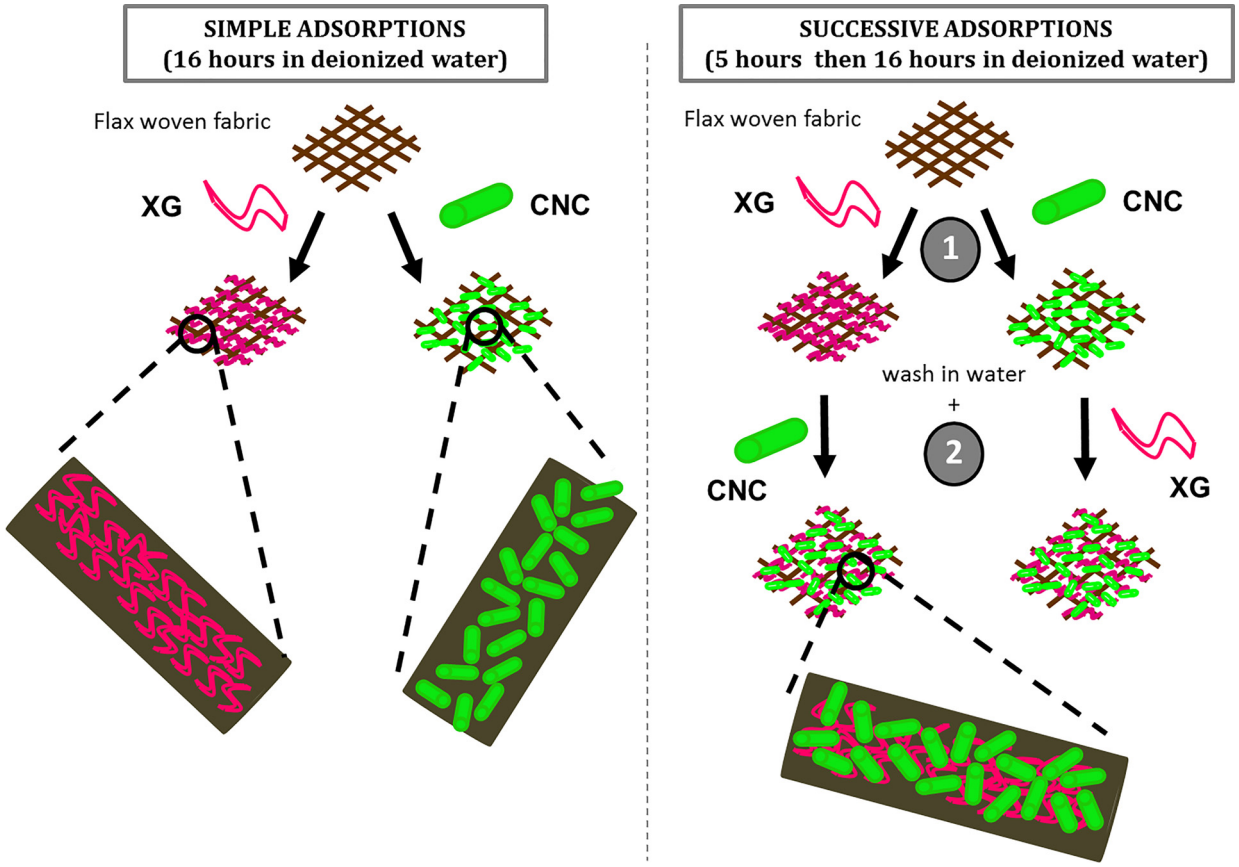


**Fig. 1.** Illustration of the different steps of adsorption processes on flax woven fabric with labeled cellulose nanocrystals (CNC) and xyloglucan (XG). For clarity reasons, XG, CNC and flax fibres are not scaled.

conditions for confocal microscopic observations. At least triplicate was performed.

*2.3.2. Successive adsorptions*

For successive adsorptions of XG / CNC-RBITC and CNC / XG-RBITC on flax woven fabrics, similar protocol as for labeled-CNC or -XG adsorption was used preceded by adsorption of XG or CNC. A solution of non-labeled XG or CNC at 0.4 g/L was added in test tubes. After 5 h, the flax woven fabrics were washed with deionized water. Labeled CNC or XG were added at concentrations ranging between 0.05 g/L and 0.45 g/L, during 16 h. Other samples were prepared with both XG-RBITC and CNC-FITC in the same conditions for confocal microscopic observations. At least triplicate was performed.

After adsorption experiments, the supernatant was collected and the absorbance of Rhodamine at 558 nm for XG-RBITC or CNC-RBITC was measured by UV spectroscopy. The amount of adsorbed XG-RBITC and CNC-RBITC on the fibres was calculated by the difference between measured absorbance in test tubes with flax woven and the absorbance of reference tubes (without flax woven).

*2.4. Scanning electron microscopy*

Elementary flax fibres extracted from the raw and treated flax woven fabrics were observed with an Environmental Scanning Electron Microscope (ESEM, FEI Quanta 200 FEG, Netherlands). The samples were pasted on an adhesive wafer and metallized in high vacuum by depositing a thin layer of carbon on their surface using a BALZERS CED 030. SEM micrographs were obtained under high vacuum at an acceleration voltage of 3 keV, a working distance of 9 mm and magnification up to 50 000 × . At least 10 micrographs per sample were performed and the most representative pictures were conserved for the discussion.

*2.5. Confocal microscopy*

The confocal microscopy images were obtained using an inverted Nikon A1 laser scanning confocal microscope. Several pieces of yarns (raw or treated) were deposited between slide and slip cover with one spacer and deionized water, avoiding the prolonged light contact. The samples were viewed with a Plan Fluor 4× or with a Plan Apo 20× Nikon objective by scanning using a laser beam at a wavelength of 488 nm and 561 nm, for imaging FITC and RBITC fluorescences respectively. The emissions of fluorescence were recorded via a photomultiplier through 500–530 nm and 570–620 nm band-pass filters, respectively. Images were processed using the NIS-Element software (Nikon). At least triplicate was performed.

*2.6. Atomic Force Microscopy (AFM)*

AFM force curves (Bruker Icon dimension) between the tip and the substrate have been performed in the air to study the adhesion between xyloglucan (XG), cellulose nanocrystals (CNC) and flax fibres. Shortly, during the adhesive force measurements, the cantilever tip approached the surface of the substrate at a speed of 1.4 µm/s until contact, and then separated. Before all these measurements, calibrations have to be performed on the cantilever Sharp Nitride Lever (SNL-10, Bruker) with a tip radius below 10 nm. First, the stiffness of the cantilever was determined by the thermal tune method and gave a spring constant of 0.098 N/m. Secondly, the sensitivity of the cantilever has to be measured. To achieve this calibration, force curves have been performed on a sapphire in contact mode. By measuring the yield of the curve, made possible by a functionality of the AFM device, the sensitivity of the cantilever can be determined. Then, the different force curves between cantilever tips and substrates were measured (Cappella & Dietler, 1999;

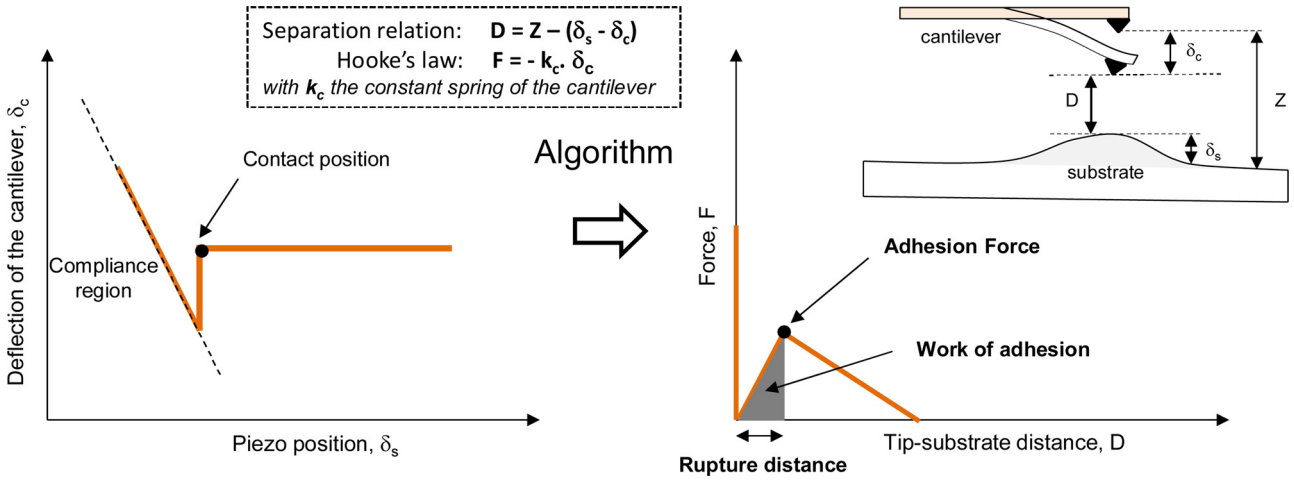


**Fig. 2.** Algorithm employed to convert the raw data graph of the force measurements obtained by AFM to the force-distance curve.

Ralston, Larson, Rutland, Feiler, & Kleijn, 2005). The raw data were converted by a calculation algorithm detailed in Fig. 2. The method is based on the conversion of the raw data graph (deflection of the cantilever vs piezo position) into a force-distance curve representing the force vs the tip-substrate distance (D). The baseline was done and the zero separation was obtained from the gradient of the constant compliance region. Different parameters are required like the cantilever rest position (Z), the deflection of the cantilever ($\delta_c$), the deformation of the surface of the substrate ($\delta_s$) and the constant spring of the cantilever ($k_c$).

In order to perform the experiments, two different tips functionalization have been done. First, one consisted on the dipping of the SNL-10 cantilever tip in a drop of XG solution at 20 g/L during 1 min and then a rinsing in water during 1 min before a drying at 60 °C during 30 min. This functionalized tip is named XG-tip within this article. The second one consisted on a tip's functionalization with CNC. The pre-coating of the tip by polycations poly(ethylene imine) (PEI, Mw = 750 000, Sigma Aldrich) was made to decrease the time of dipping and obtain a uniform coating of CNC (Kolasinska & Warszynski, 2005; Podsiadlo et al., 2007). The different steps of the dipping are described in the study of Jean, Dubreuil, Heux, and Cousin (2008)). This functionalized tip is named CNC-tip within this article. Finally, a mica substrate was also spin coated (POLO SPIN150i, SPS-Europe) by PEI and CNC following the protocol of Aulin et al. (2009), and is named CNC-surface throughout the article. Adhesion measurements were taken in contact mode at three localizations, 35 on each, i.e. 105 measurements in total for each configuration. Outliers were identified and rejected considering the interquartile range, i.e. values inferior to Q1 – 1.5 x (Q3-Q1) or superior to Q3 + 1.5 x (Q3-Q1). No obvious irreversible deformation or damaging of the substrates or the tip was detected during the measurements.

## 3. Results and discussions

### *3.1. Adsorption behavior of XG and CNC on flax woven fabrics*

In order to assess XG and CNC adsorption behaviors qualitatively and quantitatively, CNC and XG were labeled with fluorescent dies. In a first approach, confocal microscopy was used to study the localization and homogeneity of XG and CNC adsorption on flax fibres. Using the UV absorbance of the dies, the amount of XG and CNC adsorbed on flax fabrics were then used to determine adsorption isotherms.

#### *3.1.1. Microscopic observations*

Confocal microscopy images on Fig. 3 present two different views of XG-RBITC (Fig. 3a) and CNC-FITC (Fig. 3b) adsorbed on flax woven fabrics, at the scale of a yarn and an elementary fibre. Both adsorption of XG-RBITC and CNC-FITC is homogeneous with no aggregates on the surface of yarns and elementary fibres. Some microfibrils functionalized by XG-RBITC or CNC-FITC were also observed at the surface of elementary fibres. These microfibrils probably originate from the peeling of fibre cell walls and/or the presence of impurities and residues at the surface of flax fibres generated during the manufacturing process of flax woven fabrics.

Some elementary flax fibres were extracted from the yarns of treated flax woven fabrics to compare qualitatively the homogeneity of XG-RBITC (Fig. 3c) and CNC-FTIC (Fig. 3d) adsorption across flax yarns diameter. The elementary fibres collected at the outer part of flax yarns show higher intensities for both CNC-FTIC and XG-RBITC, compared to fibres extracted within the yarns. These results highlight differences in penetration of CNC-FTIC and XG-RBITC within the complex and multi-scale architecture of flax woven fabrics. Indeed the elementary fibres are twisted together to form flax yarns that are then woven to form the fabric. This puts forwards the issues related to the homogeneous treatment of industrial ligno-cellulosic substrates as natural woven fabrics having complex architectures and possibly impurities.

The surface of flax fibres treated with CNC was imaged by SEM. Cellulose nanocrystals at the surface of treated flax fibres are clearly visible in Fig. 4b (see also insert), compared to raw flax fibres (Fig. 4a) with no visible rod-like shaped nanoparticles at their surface. Adsorbed CNC appear homogeneously distributed and randomly oriented at the surface of flax fibres. This clearly demonstrated the creation of hierarchical structuration at the surface of the fibres by the formation of a nanostructured layer. This microscale structuration echoes the organization of the cellulosic elements of the flax fibres. It should be noticed that CNC were not present on all elementary fibre surfaces. This has to be related to the accessibility of fibre surfaces during adsorption treatments. Indeed, the twisted structure of flax yarns and physical contacts between elementary fibres likely limit the exposure of flax surface upon adsorption. As observed by confocal microscopy (Fig. 3), flax fibres from the inside of the yarns are less accessible and hence likely treated to a lower extent.

#### *3.1.2. Adsorption isotherms*

Xyloglucan (XG) and cellulose nanocrystals (CNC) adsorption processes are complex phenomena, and the final adsorbed amount and conformation over substrate's surface are related to several parameters such as the molar mass, concentrations, solubility, etc. (Ahola, Myllytie, Österberg, Teerinen, & Laine, 2008; Villares et al., 2015). Additionally, flax woven fabrics are industrial materials and as such are far from being model substrates. For instance, flax fibres swelling and destructuration of the fabrics occurring during treatment might influence the

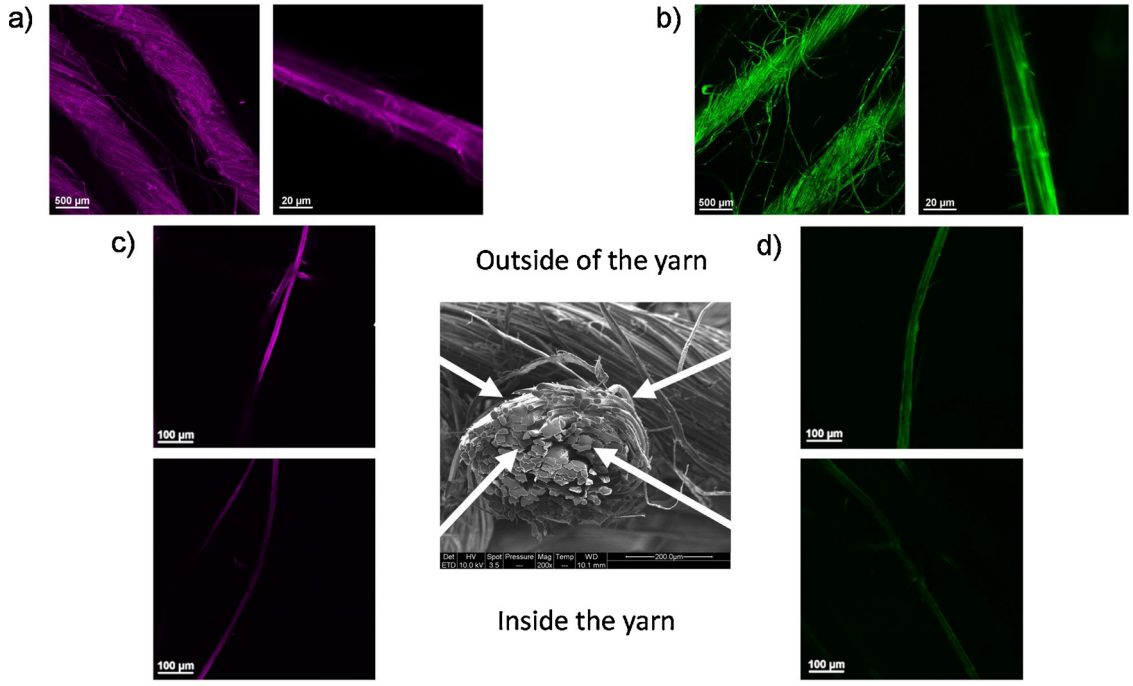


**Fig. 3.** Confocal microscopy images of (a) XG-RBITC and (b) CNC-FITC adsorption on flax yarns and elementary fibres; and of (c) XG-RBITC and (d) CNC-FITC adsorbed on elementary flax fibres extracted from different positions across the diameter of flax yarns.

adsorption kinetics. Indeed it changes the available surfaces for adsorption and their accessibility, as well as the particular microstructure of natural fibres with its porosities and the lumen. Based on preliminary adsorption trials, an adsorption time of 16 h was chosen. These trials also highlighted that further investigations on the adsorption kinetics of XG and CNC on flax fibres would be of interest.

The obtained adsorption isotherms are displayed in Fig. 5, for XG and CNC on flax woven fabrics. Adsorption was determined by comparing the UV absorbance of reference labeled CNC-RBITC or XG-RBITC solution to those incubated with flax woven fabrics. First, the Fig. 5a represents the adsorption isotherm of XG on flax woven fabrics. The insert shows the related confocal images of the yarns at low and high adsorption ratios. The difference in intensity of XG-RBITC on confocal images is nicely correlated with the increase of adsorbed amount of XG on flax fibres depending on initial concentrations of XG in solutions. A plateau is observed at average 15 – 20 mg/g. In literature, the adsorption of xyloglucan has already been studied on different ligno-cellulosic substrates. For example, paper fibres like bleached softwood kraft pulp (BSKP) (Moser, Backlund, Lindström, & Henriksson, 2018) or chemical and mechanical pulp (Zhou et al., 2006). For BSKP fibres, the amount of adsorbed XG was between 4 and 12 mg/g pulp depending on the refining time. In the case of thermomechanical pulp (TMP) and chemithermomechanical pulp (CTMP), refined or unrefined pine/spruce and birch pulp, an adsorption of XG from 15 to 30 mg/g pulp was reached. In our study, the adsorbed amount of XG on flax woven fabrics seems to be in the same range as TMP and CTMP pulps. Previous studies also reported the adsorption of xyloglucan on cellulose nanocrystals (Dammak, Quémener et al., 2015; Gu & Catchmark, 2013; Lopez et al., 2010) with a maximal adsorption between 98–333 $mg_{XG}/g_{cellulose}$. The higher amount of adsorbed XG on cellulose nanocrystals as substrates is

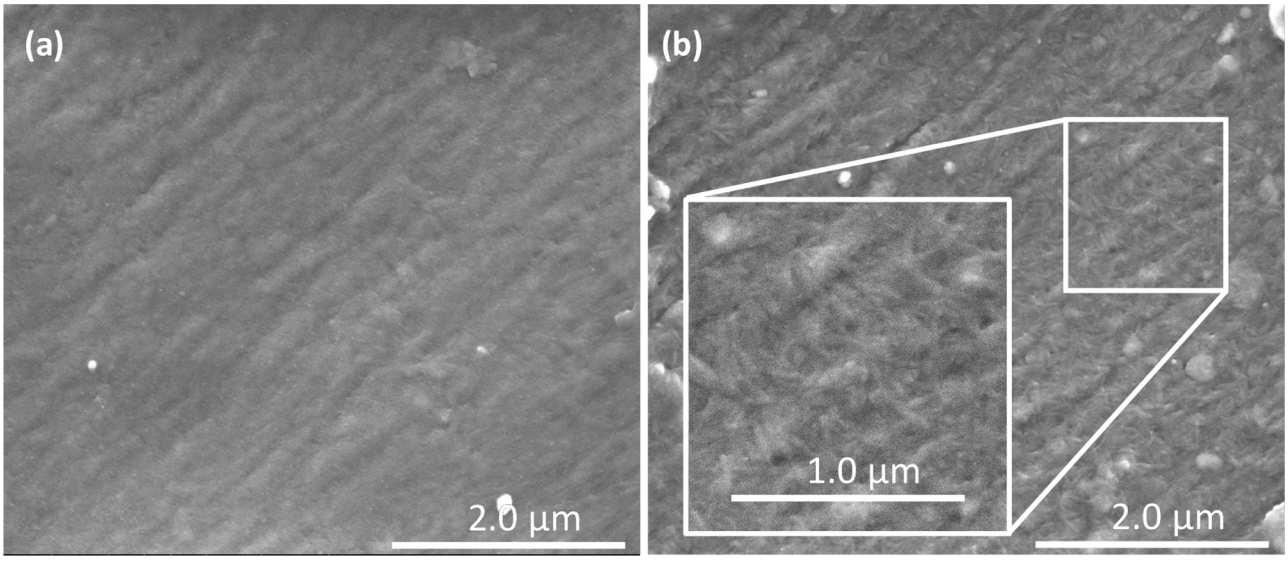


**Fig. 4.** SEM images of elementary flax fibres surface extracted from (a) raw flax woven fabrics; (b) CNC treated flax woven fabrics. (X 50 000).

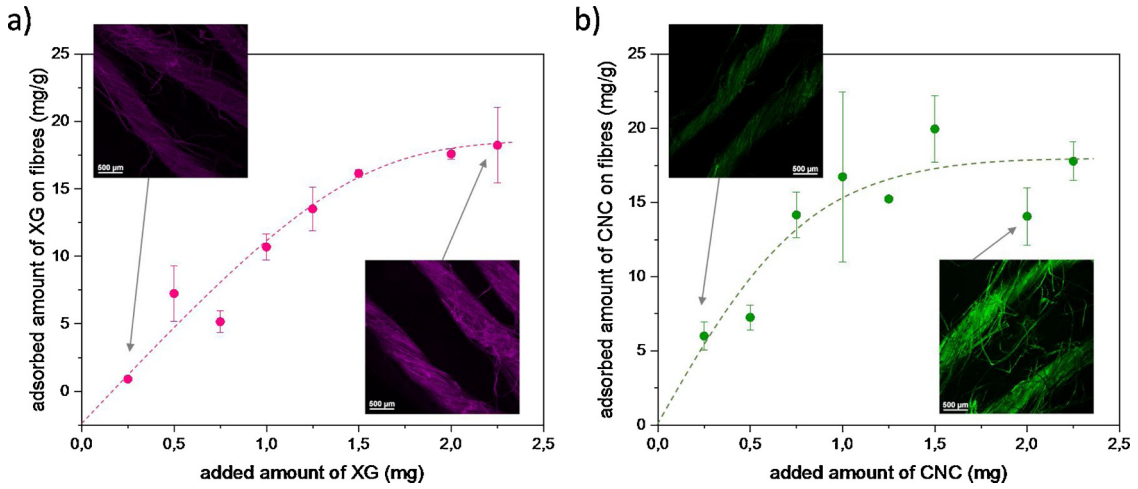


**Fig. 5.** Adsorption isotherms of (a) XG and (b) CNC on flax woven fabric and associated confocal images of XG-RBITC and CNC-FITC at low and high adsorption ratios.

due to the much higher specific surface area of CNC that range from 150 to 800 $m^2/g$ (Brinkmann et al., 2016; Habibi, 2014), as compared to that of flax fibres, roughly 1 $m^2/g$ (Bismarck et al., 2002; le Duigou, Bourmaud, Balnois, Davies, & Baley, 2012; Legras, Kondor, Heitzmann, & Truss, 2015; Müssig, Fischer, Graupner, & Drieling, 2010), even if fibre swelling could contribute to improve specific surface area.

Fig. 5b represents the adsorption isotherm of CNC on flax woven fabrics. As for XG adsorption, the difference in intensity of CNC-FITC on confocal images is well correlated with the increase amount of adsorbed CNC on flax fibres depending on initial concentrations of CNC in suspensions. A plateau is reached at average 15 – 20 mg/g. Plateau values of the amount of adsorbed XG and CNC are thus similar for the studied flax woven fabric. This points out that both XG and CNC can be adsorbed in similar quantities on flax woven fabrics, and suggests that the surface availability of the substrate has more influence on the amount of adsorbed polymers/particles than its nature and physico-chemical characteristics. It should be noticed that the adsorbed amounts of XG and CNC are rather high when considering the low specific surface area of flax woven fabric. It might be suggested that adsorption occurs in multilayered structure and not only in monolayer as usually proposed in adsorption studies based on model substrates. Other parameters than adsorption mechanisms cannot be ruled out to explain our findings. As discussed above, other processes such as the swelling of flax yarns and fibres with an increase of the available surface for adsorption, the complex and heterogeneous surface chemistry of flax fibres as well as a significant fibrillation rate due to flax processing (retting, scutching, weaving etc.) should also be considered.

### 3.2. Successive XG and CNC adsorptions on flax woven fabrics

Two different successive adsorption procedures of XG and CNC have been tested on flax woven fabrics, i.e. adsorption of XG then CNC (XG-CNC) and vice versa (CNC-XG). Both had the aim to observe a possible synergy between XG and CNC during their adsorption on flax woven fabrics.

#### 3.2.1. Microscopic observations

Fig. 6 shows confocal microscopy images of XG-RBITC (Fig. 6a) and CNC-FITC (Fig. 6b) on the same elementary flax fibre.

RBITC and FTIC were successively imaged to investigate their potential co-localization. Globally XG and CNC are homogeneously adsorbed on flax fibres, recovering the entire surface of the fibre on both Fig. 6a and b, even if some difference can be seen between the two images. As for the simple adsorptions of XG or CNC on flax woven fabrics, some microfibrils around the flax fibre are visible and are likely originated from the peeling of fibre cell walls and/or residues produced during the manufacturing process of the industrial flax woven fabric. These residues display RBITC labeling and seem thus to have a preferential adsorption of xyloglucan (Fig. 6a) than cellulose nanocrystals (Fig. 6b). The confocal plan used allows also the imaging of the inner part of the fibre. It has to be noticed that any fluorescence can be detected in the bulk of the fibres indicating that the adsorption of both XG and CNC remain located at the surface of the fibres.

Surface of XG-CNC treated flax fibres were imaged by SEM. As for simple CNC adsorption (Fig. 4), cellulose nanocrystals are clearly visible at the surface of treated flax fibres in Fig. 7b (see also insert). Adsorbed CNC appear homogeneously distributed and randomly oriented at the surface of flax fibres. As mentioned above, CNC were not present on all elementary fibre surfaces which could be explained by differences in fibre surfaces accessibility and chemistry during adsorption treatments.

#### 3.2.2. Adsorption isotherms of successive XG and CNC

Adsorption isotherms of the successive adsorptions CNC-XG and XG-CNC have been plotted in Fig. 8. The goal was to investigate if the pretreatment of flax woven fabric by CNC or XG had an influence on the adsorbed amount of the second compound (Fig. 8a; b).

It seems that the pre-adsorption of CNC on flax fibres, Fig. 8a, has no influence on the adsorption behavior of XG. Indeed, the two adsorption isotherms are very similar with the same plateau around 15 – 20 mg/g. However, it should be noticed that the plateau seems to be reached at lower initial concentrations of XG in solution with the presence of CNC on flax woven fabric. The pre-adsorption of XG on flax fibres, Fig. 8b, appears to have a slight influence on the amount of adsorbed CNC. In fact, the adsorption isotherm for XG-CNC reaches a plateau at around 25 – 30 mg/g for against 15 – 20 mg/g for simple CNC adsorption. These results demonstrate that CNC have a good affinity for flax fibres surface, the pre-adsorption of XG increasing the amount of adsorbed CNC at high initial concentration of CNC in the suspension.

### 3.3. Adhesive force measurements by Atomic Force Microscopy (AFM)

In order to get a deeper understanding of the affinity between xyloglucan (XG), cellulose nanocrystals (CNC) and flax woven fabric, we performed different adhesive force measurements by the atomic force microscopy (AFM). All of these results are detailed in Fig. 8. Different configurations tip / substrate were analyzed:

(a) *neat-tip* or *XG-tip / CNC-surface* obtained by deposition of CNC on PEI pre-coated mica substrate by spin-coating.

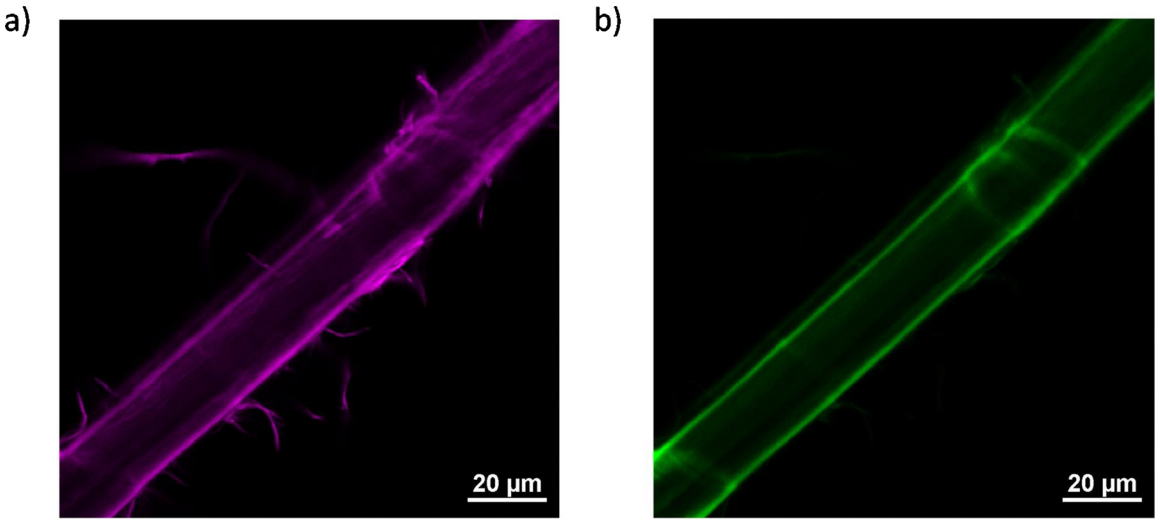


**Fig. 6.** Confocal microscopy images of successive adsorption of XG-CNC on an elementary flax fibre with (a) XG-RBITC (b) CNC-FITC.

(b) *XG-tip / flax-CNC* or *XG-tip / raw flax*, where flax-CNC corresponds to a flax fibre surface adsorbed with CNC,
(c) *CNC-tip / flax-XG* or *CNC-tip / raw flax*, where flax-XG corresponds to a flax fibre surface adsorbed with XG.

The adhesion between the tip and the substrate is due to the chemical interactions between the two surfaces into contact. The force curves measurements allow the quantification of these interactions. The rupture distance corresponds to the distance tip-substrate needed to completely separate the tip and the substrate. Finally, the work of adhesion is the energy required to separate the tip from the substrate.

All the results in Fig. 9 show high standard deviations, probably due to differences in surface roughness and chemistry between the different surfaces.

First, the configuration (a) with the neat-tip or the XG-tip approaching the CNC-surface was used as a supplementary control of the dipping of the XG-tip. The adhesion force and the work of adhesion between the XG-tip and the CNC-substrate are respectively 7 times and 25 times higher than the measurements with the untreated nitride tip. In this configuration, the rupture distance is unchanged. These results show that the XG-tip has a high adhesion force with the CNC-substrate, which is correlated with the high affinity between XG and CNC with strong hydrogen and van der Waals bonds.

Then force curves measurements were performed with the configuration (b), XG-tip in contact with the raw flax or the flax-CNC and results are detailed in Fig. 9b. We can observe that the adhesive force is the same, around 6 nN for both, with more heterogeneous measurements for the raw flax substrate (between 3 and 15 nN). The work of adhesion is also in the same range with 60–90 nN.nm. However the rupture distance seems to be slightly increased with the presence of CNC on the flax woven fabric with a maximum of 12 nm against 5 nm for the raw flax. This result shows a possible increase of the interactions zone between biopolymers XG and adsorbed CNC with the creation of an extended network. The configuration (c) is the opposite of the configuration (b), with the raw flax or flax-XG as substrates and CNC coated on the AFM tip. The adhesion force and the work of adhesion are higher between the CNC-tip and the raw flax than the flax-XG substrate with respectively 35 nN against 20 nN and 750 nN.nm against 3100 nN.nm. It means that CNC seem to have very good interactions with the flax woven fabrics, without the presence of adsorbed XG on the surface. On the other side, the rupture distance is strongly improved between the CNC-tip and the flax-XG with a median around 23 nm against 5 nm for the raw flax. That means, as observed with the configuration (b), that the interactions between CNC and adsorbed XG create specific bonds and entanglements with an extensible network, illustrated in Fig. 10. Note that adhesion force, rupture distance and work of adhesion obtained with the CNC-tip are much higher than those obtained with the XG-tip, probably because the tip coated by CNC offers

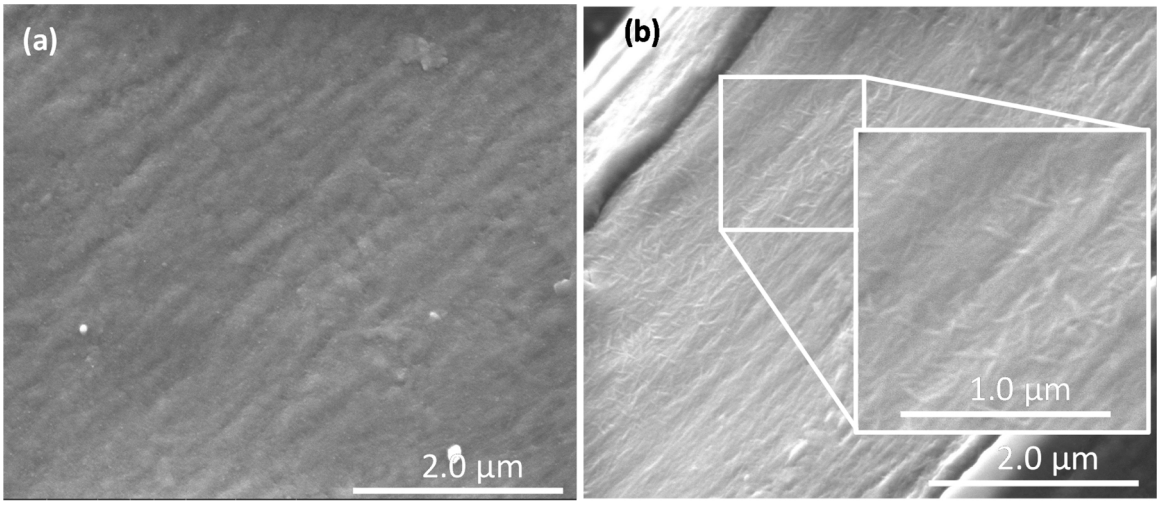


**Fig. 7.** SEM images of elementary flax fibres surface extracted from (a) raw flax woven fabrics; (b) XG-CNC treated flax woven fabrics. (X 50 000).

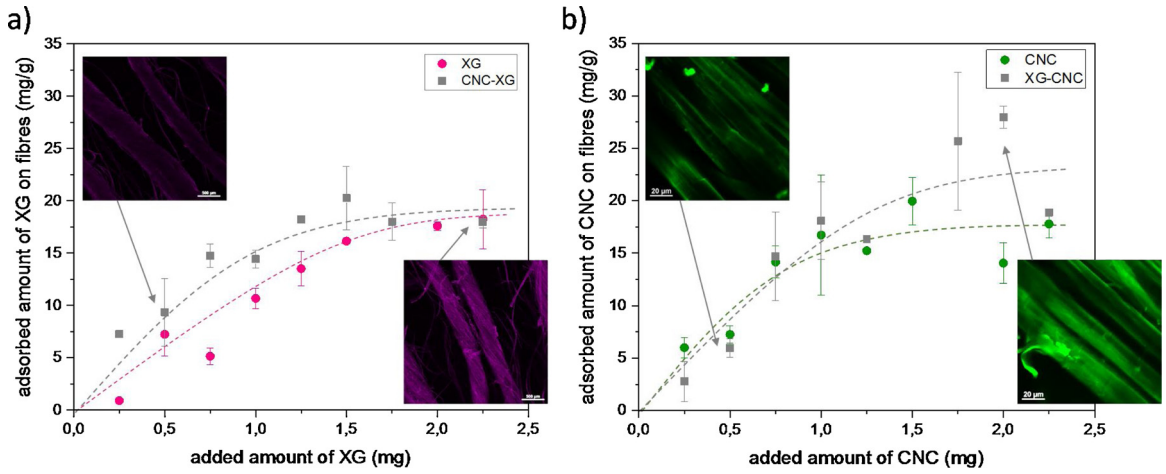


**Fig. 8.** Adsorption isotherms of (a) XG and (b) CNC for simple and successive adsorptions (XG-CNC and CNC-XG) on flax woven fabrics and associated confocal images of XG-RBITC and CNC-FITC at low and high adsorption ratios.

more available surface with more available OH groups due to the high specific surface area of CNC (more than 100 g/m$^2$) as compared to the XG biopolymer.

Despite the similar adsorbed amounts are similar for CNC and XG whatever the adsorption process, the AFM results suggest that a change in the sequence of adsorption and the combination of the two biobased building blocks can be a mean to vary the structuration of the surface organization. Accordingly, future studies will focus on the impact of hierarchically structured surfaces obtained by varying the adsorption sequence on the macroscopic properties of flax fibres based materials.

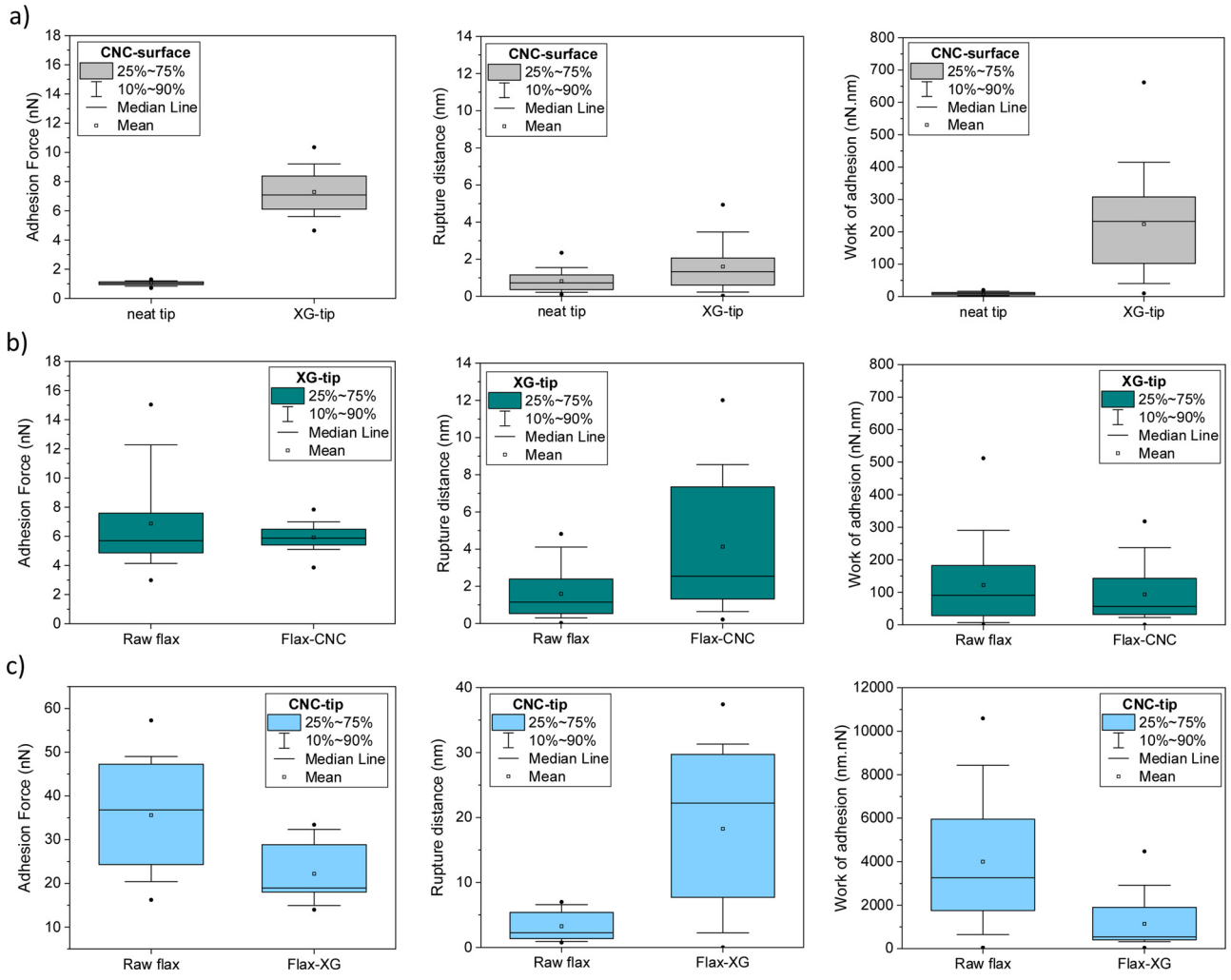


**Fig. 9.** Adhesion force, rupture distance and work of adhesion obtained with force measurements by AFM in different tip / substrate configurations (a) neat-tip or XG-tip / CNC-surface, (b) XG-tip / raw flax or flax-CNC, (c) CNC-tip / raw flax or flax-XG.

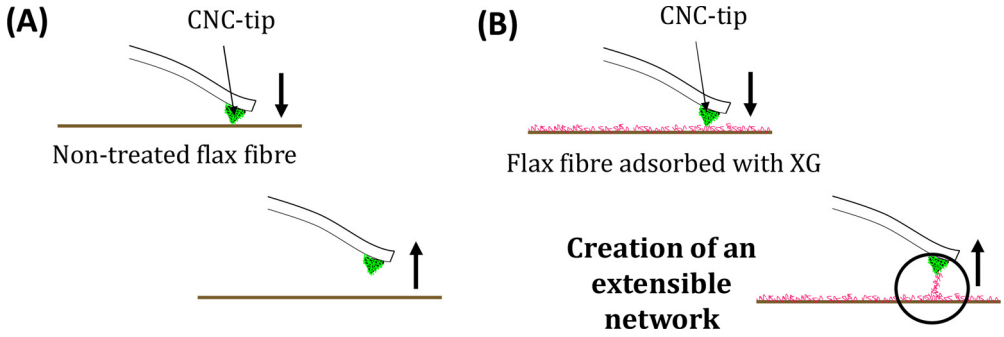


**Fig. 10.** Illustration of the adhesive force measurements by AFM with the CNC-tip when comparing substrates: (A) a non-treated flax fibre and (B) a flax fibre treated with XG.

## 4. Conclusions

Adsorption isotherms, confocal microscopy and force measurements by Atomic Force Microscopy (AFM) have been used to characterize different configurations of xyloglucan (XG) and cellulose nanocrystals (CNC) adsorptions on an industrial flax woven fabric. This industrial fabric has a complex architecture with twisted yarns composed of several hundred elementary flax fibres. Moreover, some residues likely to be generated by the manufacturing process of the fabric are present at the surface and seem to have affinities mainly with xyloglucan and also cellulose nanocrystals. The confocal images show the homogeneous distribution of XG and CNC on the flax fabric for the simple and successive adsorptions with no aggregates. However, SEM images show non-treated surfaces, which can be explained by the complex architecture of the fabric with porosities, entanglements etc. Moreover, phenomena such as swelling and destructuration occur during the dipping in water suspension and can influence the adsorption. The adsorption isotherms of XG and CNC on the flax woven fabric are very similar for the simple and successive adsorptions with a plateau around 20 $mg/g_{fibres}$, highlighting the strong influence of available surfaces on CNC or XG adsorption onto flax fibres. The pre-adsorption with XG on flax woven fabrics increases the adsorbed amount of CNC in the high concentrations and seems to change the architecture of the biopolymers network. In fact the AFM adhesive force measurements show first a good affinity between CNC and XG and also higher adhesive force and work of adhesion between CNC and the neat flax woven fabric. However, it seems that the pre-adsorption of XG on the fabric increases the rupture distance with the CNC-tip. The combined XG and CNC, adsorbed with strong interactions on the flax woven fabric, create an extensible network. These results open perspectives in the treatment of natural fibre fabrics and the possibility to change their surface and architecture with the adsorption of biopolymers like xyloglucan or nanoparticles like cellulose nanocrystals. However, we have to keep in mind the complexity of the hierarchical architecture of the industrial flax woven fabric for such treatments in terms of homogeneity, residual components and swelling effect.

## CRediT authorship contribution statement

**Estelle Doineau:** Methodology, Investigation, Funding acquisition, Writing - original draft, Writing - review & editing. **Guillaume Bauer:** Formal analysis, Methodology. **Léo Ensenlaz:** Formal analysis, Methodology. **Bruno Novales:** Investigation, Methodology. **Cécile Sillard:** Investigation, Methodology, Supervision, Validation. **Jean-Charles Bénézet:** Conceptualization, Methodology, Validation, Resources, Writing - review & editing, Supervision, Project administration. **Julien Bras:** Conceptualization, Methodology, Validation, Resources, Writing - review & editing, Supervision, Project administration. **Bernard Cathala:** Conceptualization, Investigation, Methodology, Project administration, Resources, Supervision, Validation, Visualization, Writing - review & editing. **Nicolas Le Moigne:** Conceptualization, Methodology, Validation, Resources, Writing - review & editing, Supervision, Project administration.

## Acknowledgements

Estelle Doineau thanks IMT Mines Alès and Doctoral School GAIA for funding his PhD work.

A part of this work was supported by Glyco@alps (ANR-15-IDEX-02), Idex UGA. LGP2 is part of the LabEx Tec 21 (Investissements d'Avenir – grant agreement n°ANR-11-LABX-0030) and of PolyNat Carnot Institute (Investissements d'Avenir – grant agreement n°ANR-16-CARN-0025-01).

Nadège Leray is acknowledged for her efficient help for CNC and XG labeling and adsorption experiments.

## References

Ahola, S., Myllytie, P., Österberg, M., Teerinen, T., & Laine, J. (2008). Effect of polymer adsorption on cellulose nanofibril water binding capacity and aggregation. *BioResources, 3*(4), 1315–1328.

Araújo, R., Casal, M., & Cavaco-Paulo, A. (2008). Application of enzymes for textile fibres processing. *Biocatalysis and Biotransformation, 26*(5), 332–349.

Aulin, C., Ahola, S., Josefsson, P., Nishino, T., Hirose, Y., Österberg, M., et al. (2009). Nanoscale cellulose films with different crystallinities and mesostructures—Their surface properties and interaction with water. *Langmuir, 25*(13), 7675–7685.

Benselfelt, T., Cranston, E. D., Ondaral, S., Johansson, E., Brumer, H., Rutland, M. W., et al. (2016). Adsorption of xyloglucan onto cellulose surfaces of different morphologies: An entropy-driven process. *Biomacromolecules, 17*(9), 2801–2811.

Bismarck, A., Aranberri-Askargorta, I., Springer, J., Lampke, T., Wielage, B., Stamboulis, A., et al. (2002). Surface characterization of flax, hemp and cellulose fibers; Surface properties and the water uptake behavior. *Polymer Composites, 23*(5), 872–894.

Brinkmann, A., Chen, M., Couillard, M., Jakubek, Z. J., Leng, T., & Johnston, L. J. (2016). Correlating cellulose nanocrystal particle size and surface area. *Langmuir, 32*(24), 6105–6114.

Cappella, B., & Dietler, G. (1999). Force-distance curves by atomic force microscopy. *Surface Science Reports, 34*(1-3), 1–104.

Cerclier, C., Cousin, F., Bizot, H., Moreau, C., & Cathala, B. (2010). Elaboration of spin-coated cellulose-xyloglucan multilayered thin films. *Langmuir, 26*(22), 17248–17255.

Cerclier, C., Guyomard-Lack, A., Moreau, C., Cousin, F., Beury, N., Bonnin, E., et al. (2011). Coloured semi-reflective thin films for biomass-hydrolyzing enzyme detection. *Advanced Materials, 23*(33), 3791–3795.

Cerclier, C. V., Guyomard-Lack, A., Cousin, F., Jean, B., Bonnin, E., Cathala, B., et al. (2013). Xyloglucan-cellulose nanocrystal multilayered films : Effect of film architecture on enzymatic hydrolysis. *Biomacromolecules, 14*, 3599–3609.

Christiernin, M., Henriksson, G., Lindström, M. E., Brumer, H., Teeri, T. T., Lindström, T., et al. (2003). The effects of xyloglucan on the properties of paper made from bleached kraft pulp. *Nordic Pulp and Paper Research Journal, 18*(2), 182–187.

Dai, D., & Fan, M. (2013). Green modification of natural fibres with nanocellulose. *RSC Advances, 3*(14), 4659.

Dammak, A., Moreau, C., Azzam, F., Jean, B., Cousin, F., & Cathala, B. (2015). Influence of cellulose nanocrystals concentration and ionic strength on the elaboration of cellulose nanocrystals–xyloglucan multilayered thin films. *Journal of Colloid and Interface Science, 460*(Supplement C), 214–220.

Dammak, A., Quémener, B., Bonnin, E., Alvarado, C., Bouchet, B., Villares, A., et al. (2015). Exploring architecture of xyloglucan cellulose nanocrystal complexes through enzyme susceptibility at different adsorption regimes. *Biomacromolecules, 16*(2), 589–596.

de Belder, A. N., & Granath, K. (1973). Preparation and properties of fluorescein-labelled dextrans. *Carbohydrate Research, 30*(2), 375–378.

Dick-Pérez, M., Zhang, Y., Hayes, J., Salazar, A., Zabotina, O. A., & Hong, M. (2011). Structure and interactions of plant cell-wall polysaccharides by two- and three-dimensional magic-angle-Spinning solid-state NMR. *Biochemistry, 50*, 989–1000.

Dufresne, A. (2017). *Nanocellulose : From nature to high performance tailored materials.* Walter de Gruyter GmbH & Co KG.

Faruk, O., Bledzki, A. K., Fink, H.-P., & Sain, M. (2012). Biocomposites reinforced with natural fibers : 2000–2010. *Progress in Polymer Science, 37*(11), 1552–1596.

Fortea-Verdejo, M., Lee, K.-Y., Zimmermann, T., & Bismarck, A. (2016). Upgrading flax nonwovens : Nanocellulose as binder to produce rigid and robust flax fibre preforms. *Composites Part A, Applied Science and Manufacturing, 83*(Supplement C), 63–71.

Fry, S. C. (1989). The structure and functions of xyloglucan. *Journal of Experimental Botany, 40*(210), 1–11.

Fry, S. C., York, W. S., Albersheim, P., Darvill, A., Hayashi, T., Joseleau, J.-P., et al. (1993). An unambiguous nomenclature for xyloglucan-derived oligosaccharides. *Physiologia Plantarum, 89*(1), 1–3.

Gu, J., & Catchmark, J. M. (2013). The impact of cellulose structure on binding interactions with hemicellulose and pectin. *Cellulose, 20*, 1613–1627.

Habibi, Y. (2014). Key advances in the chemical modification of nanocelluloses. *Chemical Society Reviews, 43*(5), 1519–1542.

Habibi, Y., Chanzy, H., & Vignon, M. R. (2006). TEMPO-mediated surface oxidation of cellulose whiskers. *Cellulose, 13*, 679–687.

Habibi, Y., Lucia, L. A., & Rojas, O. J. (2010). Cellulose nanocrystals : Chemistry, self-assembly, and applications. *Chemical Reviews, 110*(6), 3479–3500.

Haider, Z., Cho, H., Moon, G., & Kim, H. (2019). Minireview : Selective production of hydrogen peroxide as a clean oxidant over structurally tailored carbon nitride photocatalysts. *Catalysis Today, 335*, 55–64.

Hajlane, A., Joffe, R., & Kaddami, H. (2018). Cellulose nanocrystal deposition onto regenerated cellulose fibres : Effect on moisture absorption and fibre–matrix adhesion. *Cellulose, 25*(3), 1783–1793.

Hajlane, A., Kaddami, H., & Joffe, R. (2017). Chemical modification of regenerated cellulose fibres by cellulose nano-crystals : Towards hierarchical structure for structural composites reinforcement. *Industrial Crops and Products, 100*, 41–50. https://doi.org/10.1016/j.indcrop.2017.02.006.

Hanus, J., & Mazeau, K. (2006). The xyloglucan–cellulose assembly at the atomic scale. *Biopolymers, 82*(1), 59–73.

Hayashi, T., & Maclachlan, G. A. (1984). Pea xyloglucan and cellulose : I. Macromolecular organization. *Plant Physiology, 75*, 596–604.

Hayashi, T., Marsden, M. P. F., & Delmer, D. P. (1987). Pea xyloglucan and cellulose V: Xyloglucan-cellulose interactions in vitro and in vivo. *Plant Physiology, 83*, 384–389.

Hayashi, T., Ogawa, K., & Mitsuishi, Y. (1994). Characterization of the adsorption of xyloglucan to cellulose. *Plant & Cell Physiology, 35*(8), 1199–1205.

Idumah, C. I., Ogbu, J. E., Ndem, J. U., & Obiana, V. (2019). Infuence of chemical modification of kenaf fiber on xGNP-PP nano-biocomposites. *SN Applied Sciences, 1*(1261).

Iwakura, Y., & Okada, H. (1962). The kinetics of the reaction of organic isothiocyanates with 1-octanol in o-Dichlorobenzene. *Canadian Journal of Chemistry, 40*, 2369–2375.

Jean, B., Dubreuil, F., Heux, L., & Cousin, F. (2008). Structural details of cellulose nanocrystals/polyelectrolytes multilayers probed by neutron reflectivity and AFM. *Langmuir,* 3452–3458.

Jean, B., Heux, L., Dubreuil, F., Chambat, G., & Cousin, F. (2009). Non-electrostatic building of biomimetic cellulose－Xyloglucan multilayers. *Langmuir, 25*(7), 3920–3923.

Juntaro, J., Pommet, M., Mantalaris, A., Shaffer, M., & Bismarck, A. (2007). Nanocellulose enhanced interfaces in truly green unidirectional fibre reinforced composites. *Composite Interfaces, 14*(7–9), 753–762.

Kalia, S., Thakur, K., Celli, A., Kiechel, M. A., & Schauer, C. L. (2013). Surface modification of plant fibers using environment friendly methods for their application in polymer composites, textile industry and antimicrobial activities : A review. *Journal of Environmental Chemical Engineering, 1*(3), 97–112.

Kolasinska, M., & Warszynski, P. (2005). The effect of nature of polyions and treatment after deposition on wetting characteristics of polyelectrolyte multilayers. *Applied Surface Science, 252*(3), 759–765.

le Duigou, A., Bourmaud, A., Balnois, E., Davies, P., & Baley, C. (2012). Improving the interfacial properties between flax fibres and PLLA by a water fibre treatment and drying cycle. *Industrial Crops and Products, 39*, 31–39.

Le Moigne, N., Otazaghine, B., Corn, S., Angellier-Coussy, H., & Bergeret, A. (2018). *Surfaces and interfaces in natural fibre reinforced composites.* Springer International Publishing.

Lee, K.-Y., Bharadia, P., Blaker, J. J., & Bismarck, A. (2012). Short sisal fibre reinforced bacterial cellulose polylactide nanocomposites using hairy sisal fibres as reinforcement. *Composites Part A, Applied Science and Manufacturing, 43*(11), 2065–2074.

Lee, K.-Y., Ho, K. K. C., Schlufter, K., & Bismarck, A. (2012). Hierarchical composites reinforced with robust short sisal fibre preforms utilising bacterial cellulose as binder. *Composites Science and Technology, 72*(13), 1479–1486.

Legras, A., Kondor, A., Heitzmann, M. T., & Truss, R. W. (2015). Inverse gas chromatography for natural fibre characterisation : Identification of the critical parameters to determine the Brunauer–Emmett–Teller specific surface area. *Journal of Chromatography A, 1425*, 273–279.

Lima, D. U., Loh, W., & Buckeridge, M. S. (2004). Xyloglucan–cellulose interaction depends on the sidechains and molecular weight of xyloglucan. *Plant Physiology and Biochemistry, 42*(5), 389–394.

Lopez, M., Bizot, H., Chambat, G., Marais, M.-F., Zykwinska, A., Ralet, M.-C., et al. (2010). Enthalpic studies of xyloglucan－cellulose interactions. *Biomacromolecules, 11*(6), 1417–1428.

Malik, N., Kumar, P., Ghosh, S. B., & Shrivastava, S. (2018). Organically modified nanoclay and aluminium hydroxide incorporated bionanocomposites towards enhancement of physico-mechanical and thermal properties of lignocellulosic structural reinforcement. *Journal of Polymers and the Environment, 26*(8), 3243–3249.

Morris, S., Hanna, S., & Miles, M. J. (2004). The self-assembly of plant cell wall components by single-molecule force spectroscopy and Monte Carlo modelling. *Nanotechnology, 15*(9).

Moser, C., Backlund, H., Lindström, M., & Henriksson, G. (2018). Xyloglucan for estimating the surface area of cellulose fibers. *Nordic Pulp and Paper Research Journal, 33*(2), 194–198.

Müssig, J., Fischer, H., Graupner, N., & Drieling, A. (2010). *Testing methods for measuring physical and mechanical fibre properties (plant and animal fibres). Industrial applications of natural fibres*. John Wiley & Sons, Ltd.267–309.

Nagalakshmaiah, M., El Kissi, N., & Dufresne, A. (2016). Ionic compatibilization of cellulose nanocrystals with quaternary ammonium salt and their melt extrusion with polypropylene. *ACS Applied Materials & Interfaces, 8*(13).

Oksanen, A., Timo, R., Retulainen, E., Salminen, K., & Brumer, H. (2011). Improving wet web runnability and paper quality by an uncharged polysaccharide. *Journal of Biobased Materials and Bioenergy, 5*(2), 187–191.

Park, Y. B., & Cosgrove, D. J. (2015). Xyloglucan and its interactions with other components of the growing cell wall. *Plant & Cell Physiology, 56*(2), 180–194.

Park, Y. B., & Cosgrove, D. J. (2012). A revised architecture of primary cell walls based on biomechanical changes induced by substrate-specific endoglucanases. *Plant Physiology, 158*, 1933–1943.

Pauly, M., Albersheim, P., Darvill, A., & York, W. S. (1999). Molecular domains of the cellulose/xyloglucan network in the cell walls of higher plants. *The Plant Journal, 20*(6), 629–639.

Podsiadlo, P., Sui, L., Elkasabi, Y., Burgardt, P., Lee, J., Miryala, A., et al. (2007). Layer-by-Layer assembled films of cellulose nanowires with antireflective properties. *Langmuir, 23*(15), 7901–7906.

Pommet, M., Juntaro, J., Heng, J. Y. Y., Mantalaris, A., Lee, A. F., Wilson, K., et al. (2008). Surface modification of natural fibers using Bacteria : Depositing bacterial cellulose onto natural fibers to create hierarchical Fiber reinforced nanocomposites. *Biomacromolecules, 9*(6), 1643–1651.

Ralston, J., Larson, I., Rutland, M. W., Feiler, A. A., & Kleijn, M. (2005). Atomic force microscopy and direct surface force measurements (IUPAC Technical Report). *Pure and Applied Chemistry, 77*(12), 2149–2170.

Rastogi, V. K., & Samyn, P. (2015). Bio-based coatings for paper applications. *Coatings, 5*, 887–930.

Rusli, R., & Eichhorn, S. J. (2008). Determination of the stiffness of cellulose nanowhiskers and the fiber-matrix interface in a nanocomposite using Raman spectroscopy. *Applied Physics Letters, 93*(3), Article 033111.

Sehaqui, H., Zhou, Q., & Berglund, L. A. (2011). High-porosity aerogels of high specific surface area prepared from nanofibrillated cellulose (NFC). *Composites Science and Technology, 71*(13), 1593–1599.

Sehaqui, H., Zhou, Q., Ikkala, O., & Berglund, L. A. (2011). Strong and tough cellulose nanopaper with high specific surface area and porosity. *Biomacromolecules, 12*(10), 3638–3644.

Stiernstedt, J., Brumer, H., Zhou, Q., Teeri, T. T., & Rutland, M. W. (2006). Friction between cellulose surfaces and effect of xyloglucan adsorption. *Biomacromolecules, 7*(7), 2147–2153.

Stiernstedt, J., Nordgren, N., Wågberg, L., Brumer, H., Gray, D. G., & Rutland, M. W. (2006). Friction and forces between cellulose model surfaces : A comparison. *Journal of Colloid and Interface Science, 303*(1), 117–123.

Sun, D. (2016). Surface modification of natural fibers using plasma treatment. *Biodegradable Green Composites,* 18–39.

Villares, A., Moreau, C., Dammak, A., Capron, I., & Cathala, B. (2015). Kinetic aspects of the adsorption of xyloglucan onto cellulose nanocrystals. *Soft Matter, 11*(32), 6472–6481.

Vincken, J.-P., de Keizer, A., Beldman, G., & Gerard Joseph Voragen, A. (1995). Fractionation of xyloglucan fragments and their interaction with cellulose. *Plant Physiology, 108*, 1579–1585.

Wei, Q. (2009). 14—Emerging approaches to the surface modification of textiles. In Q. Wei (Ed.). *Surface modification of textiles* (pp. 318–323). Woodhead Publishing.

Yan, H., Lindström, T., & Christiernin, M. (2006). Some ways to decrease fibre suspension flocculation and improve sheet formation. *Nordic Pulp and Paper Research Journal, 21*(1), 36–43. https://doi.org/10.3183/npprj-2006-21-01-p036-043.

Yue, L., Maiorana, A., Khelifa, F., Patel, A., Raquez, J.-M., Bonnaud, L., et al. (2018). Surface-modified cellulose nanocrystals for biobased epoxy nanocomposites. *Polymer, 134*, 155–162.

Zhou, Q., Baumann, M., Brumer, H., & Teeri, T. (2006). The influence of surface chemical composition on the adsorption of xyloglucan to chemical and mechanical pulps. *Carbohydrate Polymers, 63*(4), 449–458.

Zhuang, R.-C., Doan, T. T. L., Liu, J.-W., Zhang, J., Gao, S.-L., & Mäder, E. (2011). Multifunctional multi-walled carbon nanotube-jute fibres and composites. *Carbon, 49*(8), 2683–2692.